EFFECT OF STREAM-WISE GROINS ON THE REDUCTION OF SHIP-WAVES ENERGY FLUX AND SEDIMENT TRANSPORTATION

J. Yagisawa
Institute for Environmental Science and Technology, Graduate School of Science and Engineering Saitama University,
Telephone: +81-48-858-3567; Fax: +81-48-858-3567
E-mail: yagisawa@mail.saitama-u.ac.jp

N. Tanaka
Institute for Environmental Science and Technology, Graduate School of Science and Engineering Saitama University

Abstract

For preventing bank erosion due to ship waves, many stream-wise groins have been installed in the downstream region of Arakawa River, Japan. However, the bank erosion still occurs at some locations even though similar-type groins are installed. In this study, field investigation at three locations on Arakawa River and numerical simulation were conducted. At each field investigation site, wave height, particle distribution of bed material and amount of sediment movement due to ship waves were measured. Amount of sediment volume increased with decreasing cross slope. As for numerical simulation on the flow around groins, total energy flux of ship waves by a ship was decreased due to installation of groins. The observed amount of bank erosion also decreased according to the decrement of the total energy flux. In addition, the amount of bank erosion increased with decreasing cross slope. These results indicate that the location with mild slope and steep slope has tendency to be accumulated or eroded, respectively, even after the groins were installed.

Keywords: *ship wave, sediment transportation, permeable groin*

1. INTRODUCTION

Waves generated by navigating ships (here after ship wave) contain a massive amount of energy that can seriously damage the coastal region (Belibassakis, 2003) and river bank(Coops et al., 1996) due to the bed degradation. From the ecological point of view, conservation of reed community around river bank has been recently attempted in Japan. Ship wave was reported to be one of the factors to decrease vegetated area of reed community (Tabata et al. , 2001). Field investigation in downstream region of Arakawa River suggested that the wash out the substrate around rhizosphere of reed plant by the progress of bed degradation behind groins is the cause of the reduction of reed community (Fukuoka et al., 1992). The researches suggested the importance of preventing bed degradation behind groins by reducing the ship wave energy for maintaining the reed community.

On the other hand, many groins have been installed in the downstream region of Arakawa River, Japan for preventing bank erosion due to ship wave. The suitable condition of groins (e.g. volumetric porosity, width, length, height and spacing of groins) for reducing wave energy have been decided by previous research (Ichikawa et al., 2004), and these values are applied at all sites in the Arakawa River. However, bank erosion still occurs at some location even after groins have been installed.According to above context, objectives of this study are to elucidate; 1) the relationship between the effect of permeable groins on the reduction of ship waves and sediment transportation characteristics, and 2) the effect of installation of groins on the change in the tendency of erosion or deposition under various cross slope conditions.

2. MATERIALS AND METHODS

2.1 MEASUMENT OF WAVE HEIGHT AND AMOUNT OF SEDIMENT TRANSPORTATION DUE TO SHIP WAVE

Field observations were conducted at three locations with different cross slope behind the groins as shown in Table 1. The wave height and amount of sediment transportation due to ship waves generated by one tanker were measured. These data were taken at the region behind the stream-wise groin. The wave heights were observed using a video technique. As shown in Figure 1(a), 10 scaled poles (Figure 1(b)) were set around groins. The still water depth (h) before coming the tanker and time variation of the wave heights were analyzed from the

Table 1 Information for each field

Location	Place-name	Distance from river mouth (km)	Cross slope	Installed year	Study item	
					Field obsevation	Numerical simulation
A	Nishi Arai	14.25	1/50	2006	○	○
B	Kawaguchi	21.75	1/25	2008	○	○
C	Higashi Yotsugi	7.50	1/80	2008	○	○
D	Motogi	14.25	1/50	2006	×	○
E	Shin Arakawa Bridge	22.40	1/10	2008	×	○
F	Kawahara	20.00	1/70	2008	×	○

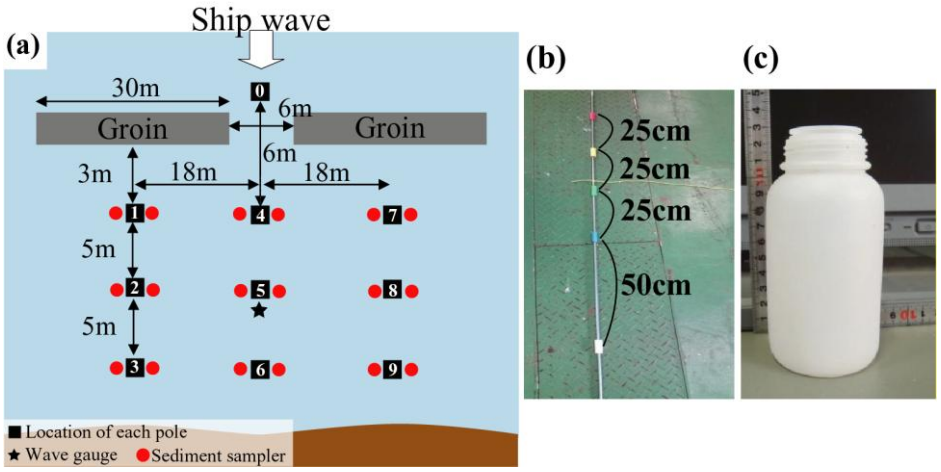

Figure 1 Experimental setup (a) Location of each pole and sediment sampler (b) scaled pole (c) sediment sampler

recorded images of the video. The accuracy of image analysis was verified by the wave heights obtained by a wave gauge located at 5 in Figure 1.

On the other hand, amount of bed load was measured by using sediment sampler set on the river bed as shown in Figure 1(c). For finding out the effect of diameter of the sediment sampler on the amount of bed load, 3 type samplers with different diameter (2.5, 3.5, 4.5 cm) were tested on field investigation site. When the diameter of sediment sampler was more than 3.5 cm, the amount of bed load became almost same. Therefore, the sampler with 3.5 cm diameter was used. In this study, two samplers were set at each location (No.1-9) as shown in Figure 1(a). The dry weight of obtained sediment in each sampler was measured using the dry kiln.

The energy flux of ship waves, E, was calculated from below equation.

$$E = \frac{1}{8}\rho g H^2 C \qquad (1)$$

$E = \frac{1}{8}\rho g H^2 C$ (1)

Where, ρ is the density of water (kg/m^3), g is the gravitational acceleration (m/s^2), H is the wave height (m), C is the wave celerity (m/s) derived from small amplitude waves theory as shown below.

$$C = \sqrt{gh} \tag{2}$$

H and h obtained from field investigation was used in Eq.(1) and Eq.(2), respectively.

2.2 GOVERNING EQUATIONS FOR SOLVING SHIP WAVE

The simulation method is used to solve numerically Boussinesq-type equations (Madsen and Sorensen, 1992) with a moving ship boundary (Chen and Sharma, 1995). Dam et al.(2006) have added the effect of energy dissipation due to wave breaking modelled by introducing the eddy viscosity terms (R_{bx} and R_{by}). In this study, drag force (f_x and f_y) due to groins are added into the momentum equations derived by Dam et al.(2006). The governing equations are shown as below.

(Continuity equation)

$$b\frac{\partial \eta}{\partial t} + \frac{\partial Q_x}{\partial x} + \frac{\partial Q_y}{\partial y} = 0 \tag{3}$$

(Momentum equation in x-direction)

$$\begin{aligned} &\frac{\partial Q_x}{\partial t} + \frac{\partial}{\partial x}\left(\frac{Q_x^2}{A}\right) + \frac{\partial}{\partial y}\left(\frac{Q_x Q_y}{A}\right) + gA\frac{\partial \eta}{\partial x} - R_{bx} + \frac{\tau_{bx}}{\rho} + \frac{f_x}{\rho} \\ &= \left(\beta + \frac{1}{3}\right)h^2\left(\frac{\partial^3 Q_x}{\partial t \partial x^2} + \frac{\partial^3 Q_y}{\partial t \partial x \partial y}\right) + h\frac{\partial h}{\partial y}\left(\frac{1}{6}\frac{\partial^2 Q_y}{\partial t \partial x}\right) \\ &\quad + \beta g h^3\left(\frac{\partial^3 \eta}{\partial x^3} + \frac{\partial^3 \eta}{\partial x \partial y^2}\right) + h\frac{\partial h}{\partial x}\left(\frac{1}{3}\frac{\partial^2 Q_x}{\partial t \partial x} + \frac{1}{6}\frac{\partial^2 Q_y}{\partial t \partial y}\right) + \beta g h^2\left\{\frac{\partial h}{\partial x}\left(2\frac{\partial^2 \eta}{\partial x^2} + \frac{\partial^2 \eta}{\partial y^2}\right) + \frac{\partial h}{\partial y}\frac{\partial^2 \eta}{\partial x \partial y}\right\} \end{aligned} \tag{4}$$

(Momentum equation in y-direction)

$$\begin{aligned} &\frac{\partial Q_y}{\partial t} + \frac{\partial}{\partial x}\left(\frac{Q_x Q_y}{A}\right) + \frac{\partial}{\partial y}\left(\frac{Q_y^2}{A}\right) + gA\frac{\partial \eta}{\partial y} - R_{by} + \frac{\tau_{by}}{\rho} + \frac{f_y}{\rho} \\ &= \left(\beta + \frac{1}{3}\right)h^2\left(\frac{\partial^3 Q_x}{\partial t \partial x \partial y} + \frac{\partial^3 Q_y}{\partial t \partial y^2}\right) + h\frac{\partial h}{\partial x}\left(\frac{1}{6}\frac{\partial^2 Q_x}{\partial t \partial y}\right) \\ &\quad + \beta g h^3\left(\frac{\partial^3 \eta}{\partial x^2 \partial y} + \frac{\partial^3 \eta}{\partial y^3}\right) + h\frac{\partial h}{\partial y}\left(\frac{1}{6}\frac{\partial^2 Q_x}{\partial t \partial x} + \frac{1}{3}\frac{\partial^2 Q_y}{\partial t \partial y}\right) + \beta g h^2\left\{\frac{\partial h}{\partial y}\left(\frac{\partial^2 \eta}{\partial x^2} + 2\frac{\partial^2 \eta}{\partial y^2}\right) + \frac{\partial h}{\partial x}\frac{\partial^2 \eta}{\partial x \partial y}\right\} \end{aligned} \tag{5}$$

Where, η is the water surface elevation. Q_x and Q_y are the depth integrated velocity components in x and y directions, respectively. t is the time, and β is the correction factor of the dispersion term (β is assumed 1/15 in this study). b is the porosity for the permeable layer of the river bed, and A is the cross-sectional area of flow in unit width under the water surface. This study applied the boundary condition for moving ship with the same equation of Chen and Sharma (1995). R_{bx} and R_{by} are calculated by using same equation with Kennedy et al.(2000) and Chen

$$\tau_{bx} = \frac{\rho g n^2}{A^{7/3}} Q_x \sqrt{Q_x^2 + Q_y^2}$$

et al.(2000). T_{bx} and τ_{by} are the shear stress acting on the bed in x and y directions and given by Eqs. (6) and (7), respectively.

(6)

$$\tau_{by} = \frac{\rho g n^2}{A^{7/3}} Q_y \sqrt{Q_x^2 + Q_y^2} \tag{7}$$

Where, n (=0.02) is the manning roughness coefficient. f_x and f_y with considering the volumetric porosity of groins (P_b=0.7) are calculated by Eqs. (8) and (9), respectively.

$$f_x = \frac{1}{2} \rho C_D (1 - P_b) \frac{Q_x |Q|}{A} \times \frac{1}{dx} \tag{8}$$

$$f_y = \frac{1}{2} \rho C_D (1 - P_b) \frac{Q_y |Q|}{A} \times \frac{1}{dy} \tag{9}$$

The drag coefficient of groin, C_d, is assumed 2.0 in this study.

2.3 SIMULATION CONDITIONS IN EACH INVESTIGATION SITE

To elucidate the relationship between the river bed change behind the stream-wise groins and energy flux of ship waves in each site, ship waves were numerically calculated at 6 locations with different cross-slope behind groins. At these 6 locations, the groins with same length, width and volumetric porosity have been installed at same interval in stream wise direction. Therefore, the cross-slope behind groins is the main parameter in this study and the effect of the slope on the reduction of energy flux of ship waves and sediment transportation can be discussed. For the numerical simulation, the grid size in both x and y direction and total stream wise length is set 1 m and 1000 m, respectively. In actual condition, river width is changed by the place. However, this study was applied to a simplified cross sectional riverbed topography as shown in Figure 2. In addition, shipping lane is fixed at 120 m from the shore line in left bank. The simplified conditions were also set in other four locations. The water level before the generation of ship waves is assumed at high tide condition and the still water depth is set 1.2 m at the location of groins. From the field investigation, representative ship was selected and it has 43.5m length, 8.5m width, 2.0 m draft and 5.3 m/s speed.

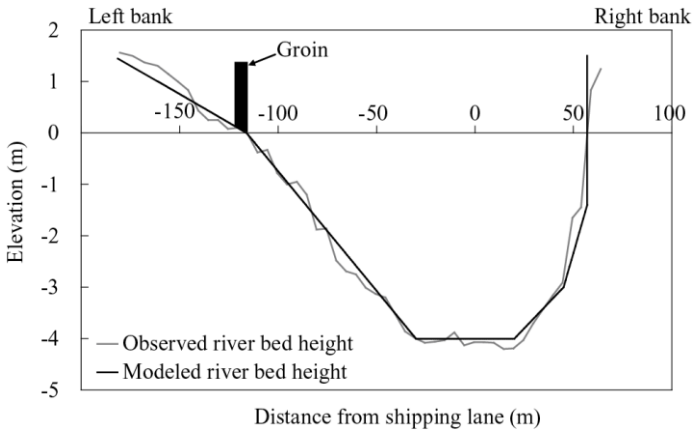

Figure 2 Observed and modelled river cross sectional shape at Location B

3. RESULTS AND DISCUSSIONS

3.1 COMPARISON BETWEEN WAVE HEIGHT OBSERVED BY WAVE GAUGE AND OBTAINED BY IMAGE ANALYSIS

In this study, ship waves were recorded by the digital video and wave height was obtained by the image analysis. To verify the applicability of this method, wave height observed by the wave gauge was compared with that obtained by the image analysis. As shown in Figure 3, the analyzed wave height can express the observed one within the reasonable limit. In other field observation site, it was confirmed that the difference with analyzed and observed wave height was around 1 cm. Therefore, the wave height obtained by the image analysis was used for calculating the energy flux of ship waves.

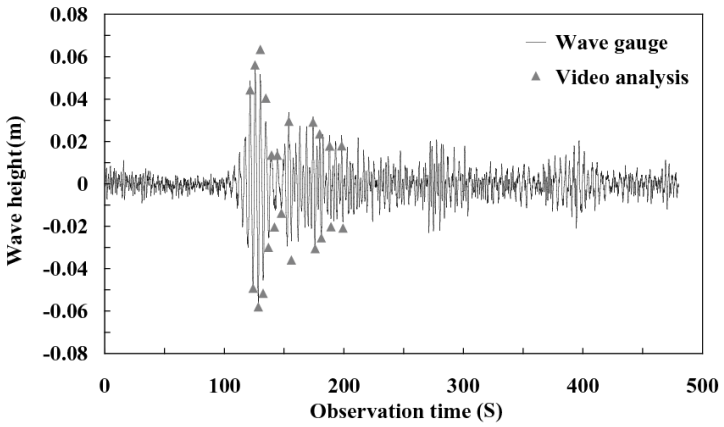

Figure 3 Comparison between observed and analyzed wave height

3.2 EFFECT OF CROSS-SLOPE BEHIND GROINS ON AMOUNT OF SEDIMENT TRANSPORTATION

Figure 4 shows the relationship between the energy flux of ship waves and amount of sediment transportation at each location. The amount of sediment transportation at Location A (with 1/50 cross slope) becomes larger than that of Location B (with 1/24 cross slope). This result suggests that the amount of sediment transportation at the location with mild slope becomes larger than that of the location with steep cross slope under the almost same ship wave condition. At Location C with milder cross slope (1/80), similar tendency can be derived as like point 1 in Figure 4. However, the amount of sediment transportation at point 2 and 3 are almost same with that of Location B (with steep cross slope). This is because a particle size of river bed material at Point 2 and 3 was bigger than that of Point 1. This result indicates that the river bed erosion around reed community is hard to occur so that a cross slope behind groins becomes mild.

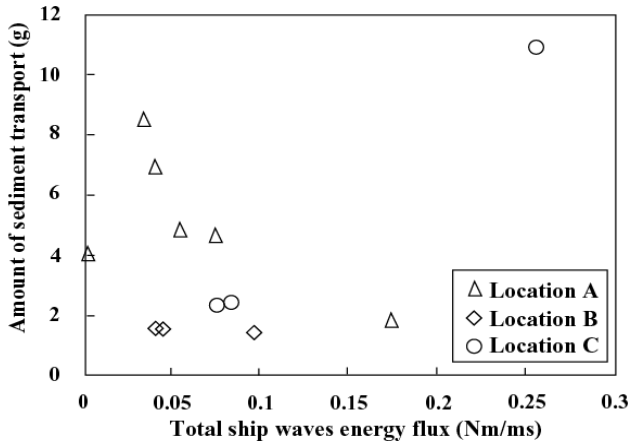

Figure 4 Relationship between total energy flux of ship waves and amount of sediment transport at three locations

3.3 VALIDATION OF NUMERICAL CALCULATION MODEL

Figure 5 shows the comparison between calculated wave height and observed one obtained at No.5 in Location 1(Figure 1). The time is defined as 0 in this figure when a ship passed at 500 m downstream from the observation location. Numerical calculation can express well 1) the timing when big wave height occurs for the first time (around 100 s), 2) the timing when the maximum wave height occurs (around 120 s), 3) the value of maximum wave height, and 4) the duration of ship waves. However, after the time when the maximum wave height is observed, the calculated value tends to greatly decrease in comparison with the observed value. Influence of the wind swell without including in this numerical calculation can be considered as this reason. The around 1 cm wave height due to wind swell was observed before coming ship wave.

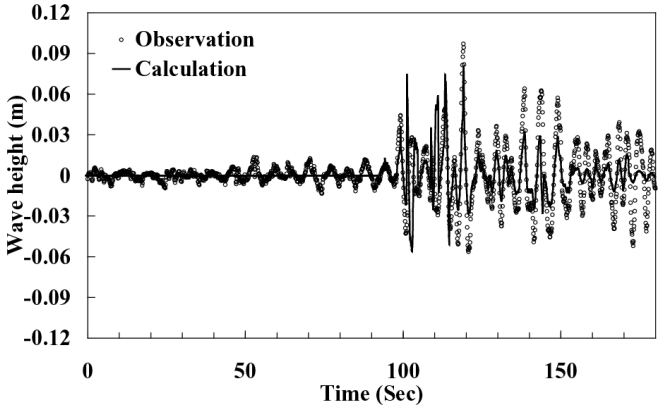

Figure 5 Verification of calculated wave height (observed wave height were obtained on No.5 at Location A)

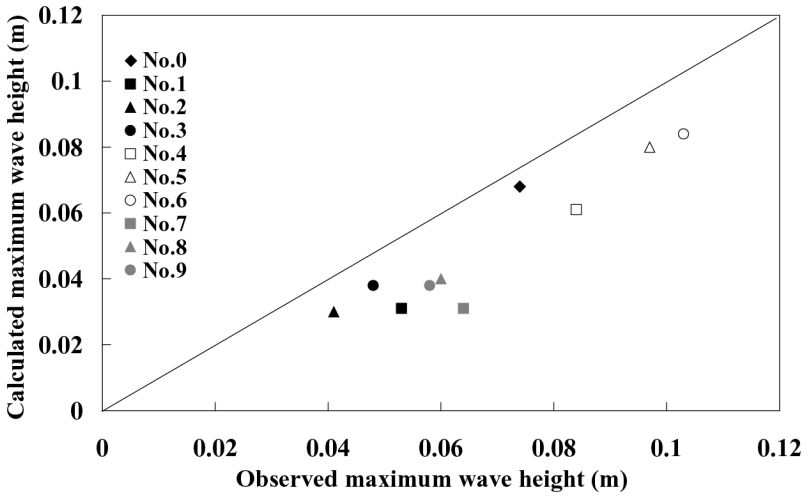

Figure 6 Comparison between calculated and observed maximum wave height (These data were obtained on No.0 – No.9 at Location A)

To validate whether this numerical simulation can calculate well the maximum wave height around groins, the result of comparison between the calculated maximum wave heights at each observation location (No.0 – No.9 in Figure 1) and observed one is shown in Figure 6. The numerical simulation can express well the maximum wave height not only at No.0 (in front of the stream-wise groin) but also at No.5 (opening mouth of two groins) and No.3 (behind the groin). According to above results, the energy flux of ship waves can be calculated by using the duration of ship wave and wave height obtained from numerical simulation.

3.4 RELATIONSHIP BETWEEN THE AVERAGE ANNUAL CHANGE OF RIVER BED TOPOGRAPHY IN CROSS SECTION AND TOTAL SHIP WAVES ENERGY FLUX AT EACH LOCATION

Figure 7 shows the relationship between the average annual change of river bed topography in cross section (here after 'C_A') and total ship waves energy flux (here after 'E_f') by passing one ship at the six locations (Location A, B, C, D, E and F in Table 1) by numerical simulation. When the values of C_A before installing groins at each location are checked, large negative C_A value can be confirmed at Location C comparing with other locations. This is supposed to be affected by the cross slope behind groins at each location. The cross slope behind groins in each location is shown in Table 1, the value of slope at Location C (mildest in six locations) and E (steepest in six locations) are 1/80 and 1/12, respectively. At Location E, the value of C_A before installing groins is smaller than other locations. This result suggests that the amount of sediment transportation at the location with mild cross slope becomes larger than that of the location with steep cross slope. This tendency is confirmed from field investigation.

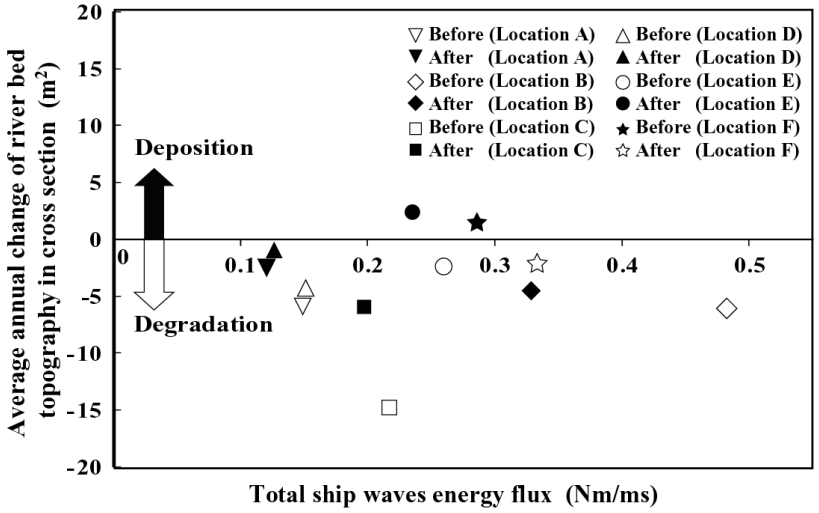

Figure 7 Relationship between the observed average annual change of river bed topography in cross section and simulated total energy flux of ship waves by a ship at six locations

On the other hand, from the comparison between C_A values before and after installing the groins, the different effect of the groins insulation on the change of river bed topography behind groins can be found. At the Location B with steep cross slope, the erosion continues although the tendency of erosion weakens after installing groins. In contrast, at the Location F with mild cross slope, the value of C_A becomes positive (it means deposition) after installing groins, although the C_A is negative before installing groins. When the variations of C_A before and after installing groins at Location C and E are compared, the variation of C_A at the location with mild cross slope (as like Location C) is larger than that of the location with steep cross slope (as like Location E). At these six locations, the groins have been installed as same length, width, volumetric porosity and setting interval in stream wise direction. However, the cross slope

behind groins affects the tendency to erosion or deposition as shown in Figure 7. This indicates that it is necessary to change the structure of groins (e.g. volumetric porosity) depending on the cross slope for preventing the erosion behind groin.

4. Conclusion

The following conclusions and recommendations were obtained by this study:

1) The amount of sediment transportation at the location with mild slope becomes larger than that of the location with steep cross slope under the almost same ship wave condition.

2) It is necessary to change the structure of groins (e.g. volumetric porosity) depending on the cross slope for preventing the erosion behind groin.

References

Bonham AJ.: The management of wave-spending vegetation as bank protection against boat wash, *Landscape and Urban Planning* 10(1), pp.15-30, 1983.

Belibassakis, K.A.: Coupled-mode technique for the transformation of ship-generated waves over variable bathymetry regions, *Applied Ocean Research*, 25, pp.321–336, 2003.

Chen, X.N. and Sharma, S.D.: A slender ship moving at a near-critical speed in a shallow channel, *J. Fluid Mech.*, 291, pp.263-285, 1995.

Chen, Q., Kirby, J.T., Dalrymple, R.A., Kennedy, A.B. and Chawla, A.: Boussinesq modeling of wave transformation, breaking and runup. 2: 2D. *J. of Waterway, Port, Coastal, and Ocean Engineering*, 126(1), pp.48-56, 2000.

Coops, H., Geilen, N., Verheij, H.J., Boeters, R. and Velde, G.: Interactions between waves, bank erosion and emergent vegetation: an experimental study in a wave tank, *Aquatic Botany*, 53, pp.187-198, 1996.

Dam, K.T., Tanimoto, K., Ngueyn B.T. and Akagawa, Y.: Numerical study of propagation of ship waves on a sloping coast, Ocean Engineering, 33, pp.350-364, 2006.

Fukuoka, S., Kohmura, K., Watanabe, A. and Miura, H.: Effect of marsh reeds in the river on the energy dissipation of boat-generated waves, Annual journal of hydraulic engineering JSCE, 36, pp.713-718, 1992. (in Japanese with English abstract)

Ichikawa, Y., Oshima, Y and Maruta, E.: A study on the effect of ship waves in the lower Ara River, Report of Riverfront Research Institute, 15, 150-156, 2004. (in Japanese with English abstract)

Kennedy, A. B., James, Q. C., Kirby, T. and Dalrymple, R.A.: Boussinesq modeling of wave transformation, breaking, and runup, 1: 1D. *J. of Waterway, Port, Coastal, and Ocean Engineering*, 126(1), pp.39-47, 2000.

Madsen, P.A. and Sørensen, O.R.: A new form of the Boussinesq equations with improved linear dispersion characteristics. Part 2. A slowly-varying bathymetry, *Coastal Engineering*, 18, pp.183–204, 1992.

Tabata, K., Ote, T., Eagmi, K., Hirata, S. and Fukuoka, S.: Conservation and formation of reed-beds at the lower reaches of Arakawa River, Advanced river engineering, 7, pp.273-278, 2001. (in Japanese with English abstract)